Journal of Environmental Management 223 (2018) 703–712

Contents lists available at ScienceDirect

Journal of Environmental Management

journal homepage: www.elsevier.com/locate/jenvman

Research article

Combined effects of polyacrylamide and nanomagnetite amendment on soil and water quality, Khorasan Razavi, Iran

Mohammadreza Roshanizarmehri[a], Amir Fotovat[a,*], Hojat Emami[a], Martin Kehl[b], Daniel R. Hirmas[c], Mohsen Hosseinalizadeh[d], Navid Ramezanian[e]

[a] Department of Soil Science, Faculty of Agriculture, Ferdowsi University of Mashhad, Mashhad 91775-1163, Iran
[b] Institute of Geography, University of Cologne, Albertus-Magnus-Platz, 50923, Cologne, Germany
[c] Department of Environmental Sciences, University of California–Riverside, Riverside, CA 92521, USA
[d] Department of Watershed & Arid Zone Management, Gorgan University of Agricultural Sciences and Natural Resources, Gorgan 49189-4346, Iran
[e] Department of Chemistry, Faculty of Science, Ferdowsi University of Mashhad, Mashhad 91775, Iran

ARTICLE INFO

Keywords:
Anionic polyacrylamide
Nanomagnetite
Water quality
Soil erosion
Aggregate size

ABSTRACT

Nanotechnology is increasingly being used to remediate polluted soil and water. However, few studies are available assessing the potential of nanoparticles to bind surface particles, decrease erosion, and minimize the loading of water pollutants from agricultural surface discharge. To investigate this potential, we treated in situ field plots with two practical surface application levels of anionic polyacrylamide (PAM only) with and without nanomagnetite (PAM-NM), examined soil physical properties, and evaluated the impact of this amendment on contaminant sorption and soil erosion control. Polyacrylamide and PAM-NM treatments resulted in 32.2 and 151.9 fold reductions in Mn^{2+}, 1.8 and 2.7 fold for PO_4^{3-}-P, and 2.3 and 1.6 fold for NH_4^+-N, respectively, compared to the control. Thus, we found that the combination of PAM and NM, had an important inhibitory effect on NH_4^+-N and PO_4^{3-}-P transport from soil—pollutants which can contribute substantially to the eutrophication of surface water bodies. Additionally, since the treatment, especially at a high concentration of NM, was effective at reducing Mn^{2+} concentrations in the runoff water, the combination of PAM and NM may be important for mitigating potential risks associated with Mn^{2+} toxicity. Average sediment contents in the runoff monitored during the rainfall simulation were reduced by 3.6 and 4.2 fold for the low and high concentration PAM-NM treatments when compared to a control. This treatment was only slightly less effective than the PAM-only applications (4.9 and 5.9 fold, respectively). We report similar findings for turbidity of the runoff (2.6–3.3 fold for PAM only and 1.8–2.3 fold for PAM-NM) which was caused by the effects of both PAM and NM on the binding of surface particles corresponding to an increase in aggregate size and stability. Findings from this field-based study show that PAM-modified NM adsorbents can be used to both inhibit erosion and control contaminant transport.

1. Introduction

Soil erosion and contaminant transport are among the processes that most threaten the quality of soil and water resources in Iran (Jahanjo, 2000; Agheli-e Kohneshari and Sadeghi, 2005; AQUASTAT, 2008). Contamination levels in runoff water can greatly affect surface water toxicity and, thus, the health of aquatic ecosystems (Reimer, 1999; ESRD, 2014). In addition, soil erosion diminishes soil fertility (Noor et al., 2013; Fu and Chen, 2000; Mafongoya et al., 2006), reducing the water-storage capacity of reservoirs (Rahmanian and Banihashemi, 2011; Wisser et al., 2013) and causing eutrophication (Jennings et al., 2003; Uwimana et al., 2017) as sediments and nutrients are lost by agricultural runoff and transported downstream. In Iran, reservoirstorage volume reduction is 1.65% annually, more than the average annual loss in the world (0.96%) (ICOLD Committee, 2009). Eutrophication of the Torogh reservoir in Iran, which supplies drinking water to approximately 3.4 million people in Mashhad, Khorasan Razavi Province, and supports agricultural irrigation in the area, is due to extensive use of fertilizers in the associated basin and subsequent erosion and runoff (Heydarizad, 2018). Thus, better environmental management strategies are required given the extent of soil and water contamination in this region. In particular, the development of new

* Corresponding author.
E-mail addresses: roshanizarmehri@mail.um.ac.ir (M. Roshanizarmehri), afotovat@um.ac.ir (A. Fotovat), hemami@um.ac.ir (H. Emami), kehlm@uni-koeln.de (M. Kehl), daniel.hirmas@ucr.edu (D.R. Hirmas), mhalizadeh@gau.ac.ir (M. Hosseinalizadeh), ramezanian@um.ac.ir (N. Ramezanian).

https://doi.org/10.1016/j.jenvman.2018.06.061
Received 25 December 2017; Received in revised form 14 June 2018; Accepted 18 June 2018

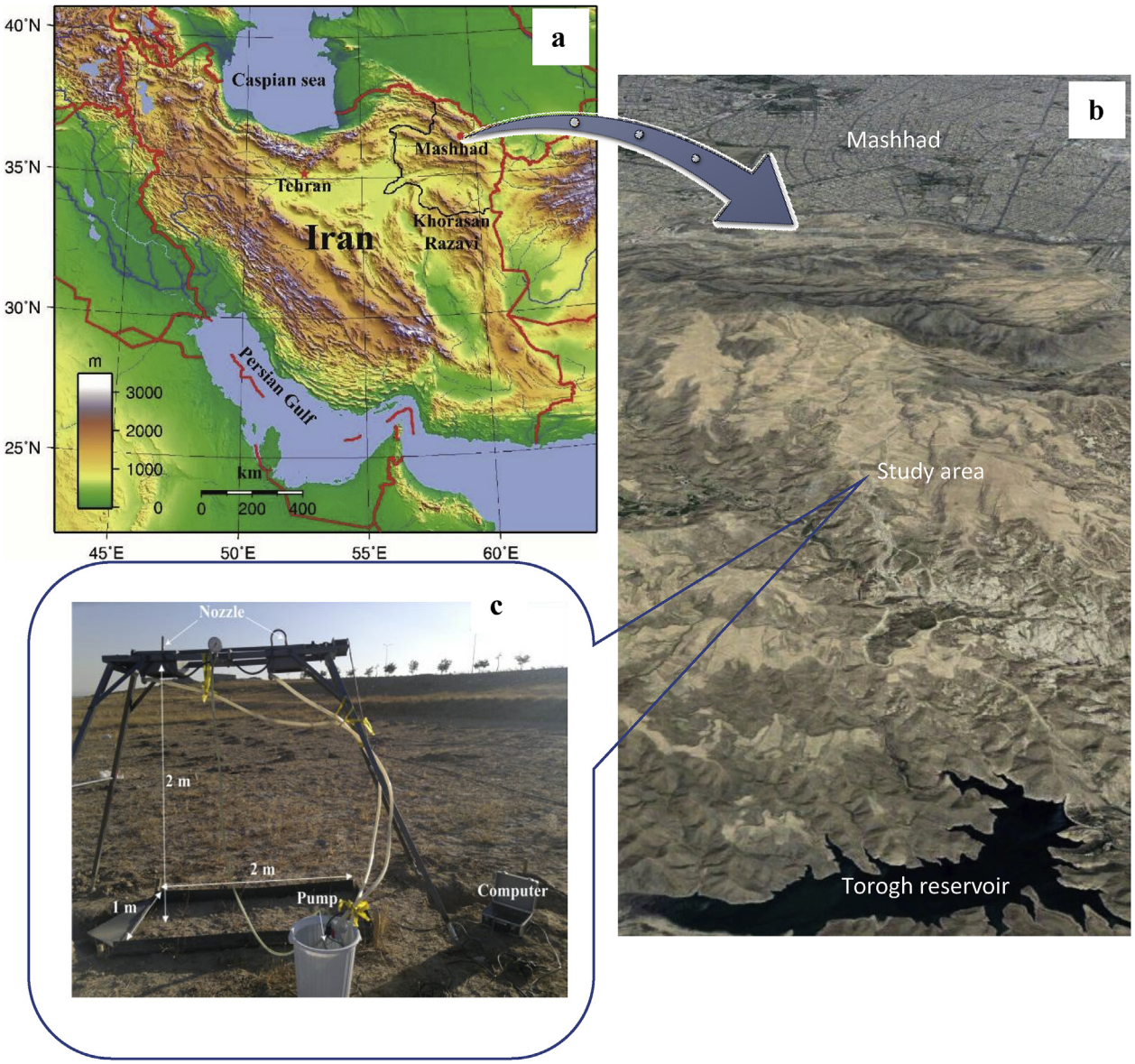

Fig. 1. (a) General shaded relief map of Iran showing the location of Khorasan Razavi (Sadalmelik, 2007). (b) Oblique image showing the location of the study area in relation to the Torogh reservoir and the City of Mashhad (Source: 36°12′22.50″ N and 59°32′35.81″ E, Google Earth, image date: 20 April 2018; accessed 10 June 2018). (c) Photograph of the rainfall simulator and experimental setup.

strategies and/or technology for the combined management of soil erosion and runoff contamination is crucial for mitigating future degradation of soil and water quality in this region.

A variety of methods have been employed to minimize nutrient concentration in runoff, reduce water and sediment discharge, and protect soil from erosive forces through the creation and maintenance of soil aggregates which serve to stabilize the surface via increased interaggregate particle-to-particle binding strengths (Orts et al., 2007) and intraaggregate pore networks, which improve infiltration, reduce runoff and, thus, sediment load (Mamedov et al., 2007). One such technology employs non-oil polymeric mulches, such as acrylamide-based polymers, because of its low cost and soil fertility benefits (Kurenkov and Myagchenkov, 1996; Sojka et al., 2007). Water-soluble cationic and neutral polyacrylamides are toxic and are usually avoided in environmental applications but the anionic polyacrylamide (PAM) $[(H_2{-}CH{-}CO{-}NH_2)_n]$ used in agriculture is generally considered environmentally safe (Seybold, 1994; Entry et al., 2002; Sojka and Entry, 2000; Sojka et al., 2007; Weston et al., 2009) as evidenced by its wide use in the food industry, mineral processing, and municipal water treatment as a settling agent (Barvenik, 1994).

The molecular properties (large molecular weight and charge density) of PAM allow it to be used to effectively flocculate clay particles, stabilize soil aggregates, diminish the formation of surface sediment seals, mitigate erosion, increase plant available water, improve drainage, and enhance the removal of salts, nutrients, pesticides, microorganisms, and weed seeds from water and runoff (Green et al., 2000; Sojka et al., 2004; Sivapalan, 2006; Sparks, 2007; Blanco and Lal, 2008) and as a consequence, improve water quality (Ajwa and Trout, 2006; Guzzo and Guezennec, 2015). Polyacrylamide strengthens the bonds between soil particles through coulombic and van der Waals forces (Orts et al., 2007). Effectiveness of PAM, however, depends on a number of factors including soil texture, rainfall and runoff characteristics, soil management, mineralogy and extractable Fe (McLaughlin and Bartholomew, 2007; Blanco and Lal, 2008).

In recent years, magnetite nanoparticles have received attention as a new soil remediation technology due to its strong affinity for heavy metals and nutrients, high magnetic susceptibility, non-toxicity, biocompatibility, low cost of production and chemical stability over a wide

pH range (Wu et al., 2008; Street et al., 2014). When combined with PAM, these nanoparticles have also been applied to soil to effectively reduce erosion and runoff while increasing water infiltration (Zheng, 2011). In order to prevent flocculation during the application of nanoparticles, a stabilizer such as PAM is often used (He and Zhao, 2005; He et al., 2007; Liang et al., 2013).

The overall objective for this study was to evaluate the effects of a combined PAM and NM soil amendment on controlling erosion, runoff, and the transport of NH_4^+-N, PO_4^{3-}-P, and Mn^{2+} in Khorasan Razavi province, Iran. This region is particularly important as it contains the Torogh reservoir, a major drinking and agricultural water source with a surrounding area that has had 2200 tons $year^{-1}$ of manure and 100 tons $year^{-1}$ of chemical fertilizers applied to improve soil fertility (Tabrizi and Ghorbani, 2013). In addition, this region of Iran is representative of the larger regional erosional processes that are driven by infrequent but intense rainfall events, sparse plant cover, high application rates of fertilizers, and dispersive soil environments. Due to the high costs of off-site water treatment, the use of in situ field amendments for the simultaneous control of soil erosion and on-site nutrient leaching is essential.

2. Materials and methods

2.1. Study area

The study area is located in an agricultural field to the southeast of the city of Mashhad in Khorasan Razavi Province, Iran, in the foothills of the Khalaj Mountains with an average of 227 mm of annual precipitation. This area is part of the northern Binalood range, which is located within the river basin of the Torogh reservoir (Fig. 1a–c). The field was left fallow for the previous 5 years. The dominant vegetation cover is composed of pasture plants such as *Artemisia* sp., *Astragalus* sp., and *Poa* sp., and there is dry-land farming in some low-pitched foothills. Agriculture, pasture, and recreation are the main management systems. Based on U.S. Soil Taxonomy (Soil Survey Staff, 2014), soils in the study area are classified as Aridisols.

2.2. Field experiments

We used plot-level field experiments in order to generalize our findings to natural conditions. A total of 21 1 × 2-m plots were placed in the agricultural field in locations where similar slopes and plant cover and residues were identified. The data of 15 of these plots were used for runoff, sediment concentration, turbidity and erosion rate measurements. Land-surface gradients with 3% slopes measured from 2.5-m slope lengths and plant cover and residues (slight cover of agropyron) comprising approximately 4% of the plot were used as the criteria for plot locations. Plots were oriented with their long dimension downslope, spaced with a minimum distance of 1.5 m, and framed with a 12-cm tall steel flange that was carefully hammered into the ground until only 7 cm was exposed. This frame was used to collect runoff and sediment during the rainfall simulation. Three soil samples were collected from the upper 15 cm layer between the plots and aggregated to assess the soil surface particle-size distribution (PSD) of the field. In addition, one representative intact sample from each treatment was selected to examine the aggregate-size distribution (ASD) with depth.

Treatments were applied to the plots in triplicate as follows: (A) control; (B) 1.25 g m^{-2} PAM; (C) 2.5 g m^{-2} PAM; (D) 1.25 g m^{-2} PAM + 0.05 g m^{-2} NM particles; (E) 2.5 g m^{-2} PAM + 0.05 g m^{-2} NM particles; (F) 1.25 g m^{-2} PAM + 0.1 g m^{-2} NM particles; (G) 2.5 g m^{-2} PAM + 0.1 g m^{-2} NM particles. We used a high-molecular-weight (15 Mg mol^{-1}) PAM solution in these treatments obtained from Aquatech Company (GFLOC A800, Switzerland). In order to create similar initial soil moisture conditions in all plots, 2.5 and 5 g of dry PAM, separately, were dissolved in 10 L of distilled water one day before the rainfall simulation, stirred for 4 h, and sprayed uniformly onto the appropriate plots (Shoemaker, 2009; Zhang et al., 2010; Lee et al., 2011). The nanomagnetite particles were synthesized by a co-precipitation method described below. Small soil clods (~2 cm in diameter) were sampled from three locations within one plot from each treatment to assess treatment effects on soil ASD. One of these clods from the control plot was selected for further soil organic carbon (SOC) analysis. In addition, a small clod was sampled beside each plot to assess initial soil moisture.

The rainfall simulator used in this study consisted of a steel pipe that supported two nozzles located 2 m above the ground surface of the plot. The nozzles were connected to a solenoid and a pressure gauge that allowed the water to be delivered under constant pressure. A computer connected to the solenoid controlled the angle, number of pulses per nozzle, and time of water shutoff. Local groundwater was used in the rainfall simulator and applied at a constant rainfall intensity of 103 mm h^{-1} based on the intensity-duration-frequency curve for this region (Alizadeh, 1995) under a pressure of 60 kPa for a duration of 30 min.

Christiansen's uniformity coefficient (Christiansen, 1942; Dabbous, 1962) was used to assess uniformity of water application beneath the rainfall simulator. The coefficient is an index that relates the sum of the deviation of volumes from individual measurements under the rainfall simulator to the total volume of water applied with a value of 100% representing perfect uniformity and values less than 100% indicating non-uniformity in application. A range from 80 to 100% is generally considered an acceptable rainfall uniformity (Zheng, 2011).

Runoff samples were collected in 5-min intervals from the start of the rainfall simulation for a total of 30 min. For each simulation, the time to runoff initiation was recorded as the time between the start of the simulated rainfall and the beginning of runoff collection. Runoff volumes from each sample were measured in the field and a well-mixed 1-L subsample was collected for further analysis in the laboratory. In addition, the remaining sediment was collected for ASD determination in the laboratory.

2.3. Laboratory analyses

The local groundwater used in the rainfall simulations and the elemental concentration in the soil were analyzed by inductively coupled plasma – optical emission spectroscopy (ICP-OES, GBC, PerkinElmer, Market-Shimadzu) for Ca^{2+}, Mg^{2+}, and Na^+ to calculate sodium adsorption ratios (Sparks, 2003). Bicarbonate and chloride were measured by titration with 0.01 M H_2SO_4 and 0.01 M $AgNO_3$, respectively. After filtering runoff samples through a 0.45 µm millipore filter paper, Mn^{2+}, PO_4^{3-}-P and NH_4^+-N concentrations, were measured by inductively coupled plasma mass spectrophotometry (Thermo Scientific X Series 2 ICP-MS), spectrophotometer (UV/VIS S 2000), and kjeldahl (Kjeltec 2300, Foss Tecator. Sweden), respectively. In addition, we measured EC and pH from an aliquot of the groundwater sample in the laboratory.

The 1-L runoff samples from each interval were analyzed for turbidity (Lovibond TB 210 IR Turbidity Meter, Tintometer GmbH, Dortmund, Germany) at 0, 5, 10, 15, 20, 25, and 30 min, and 1, 3, 5, 7, and 9 days after mixing by transferring 5 mL of the suspension obtained approximately 10 cm below the liquid surface to a glass vial. The 5-mL aliquot was returned to the 1-L container after being analyzed in the turbidity meter. The sediment in the 1-L sample was separated through filtration, dried at 105 °C for 24 h, and weighed to obtain the total sediment mass in the sample. The total runoff volume measured in the field was used to calculate the total sediment mass eroding from the plot during the sampling intervals of the rainfall simulation. The remaining sediment sample collected in the field from each sampling interval was air-dried, aggregated in equal proportions by 10-min intervals, and analyzed by laser diffraction (LS 13 320 Series, Beckman Coulter, Indianapolis, IN) in deionized water without pretreatment in order to examine the ASD of each sample (Klopfenstein et al., 2015).

The aggregated soil sample taken in the field was pretreated with hydrogen peroxide to remove organic matter, dispersed in a 1 M NaOH and 10% $(NaPO_3)_6$ solution (McTainsh et al., 1997), and analyzed by laser diffraction. In addition, soil samples taken to examine ASD from each treatment were sectioned into 3 layers corresponding to depths of 0–3, 3–6, 6–10 mm and analyzed by laser diffraction without pretreatment. Soil organic carbon was taken as the difference between total and inorganic carbon measured by coulometry (Engleman et al., 1985; Jackson and Roof, 1992) from a small clod sampled in one of the control plots prior to the rainfall simulation. Soil water content samples were measured gravimetrically.

2.4. Preparation of the PAM-NM composite

Polyacrylamide-bridged magnetite nanoparticles were prepared as follows. Iron salts (0.001 M $FeSO_4$ and 0.002 M $FeCl_3$) were dissolved in deoxygenated deionized water to prepare a ferrous-ferric stock solution at room temperature (21 ± 1 °C) and pressure. Under N_2 purging, the ferrous-ferric stock solution was mixed with the appropriate PAM solution as described above. A solution of 2 M NaOH was added dropwise to the solution until a pH value of about 11 was obtained. A color change to black indicated the formation of the nanoparticles. The suspension was sealed and placed in a dark room for 12 h in order to allow the magnetite nanoparticles to grow. The pH value was lowered to ~7 with 2 M HCl (Schwertmann and Cornell, 2000; Zheng, 2011) and the suspension (PAM-bridged NM) was used within one hour of synthesis. The NM particles and PAM modified NM were analyzed by Fourier-transform infrared spectroscopy (FT-IR) (Tensor27, Bruker Germany). The morphology of the Fe_3O_4 particles coated by PAM were measured from micrographs obtained by field-emission scanning electron microscopy (FESEM) (TESCAN MIRA3-FEG) and X-ray diffractometer (XRD) equipped with a graphite crystal monochromator using CuKα radiation (Rigaku-D/max-2500, Japan). Samples were examined in the °2θ range of 2–60 with a scanning step of 0.02 and a 6 s $step^{-1}$ counting time.

2.5. Data analysis

The rate of erosion (E_r) was calculated as (Shoemaker, 2009):

$$E_r = \frac{TS_C \times V_R}{T \times A} \quad (1)$$

where TS_C is the total sediment concentration, V_R is the runoff volume, T is the sampling interval (i.e., 5 min), and A is the plot area (i.e., 2 m^2). Statistical analyses were conducted using Origin 8.5 (OriginLab Corporation, Northampton, MA).

3. Results and discussion

3.1. Characterization of Fe_3O_4 (NM particles) and PAM-NM composite

The XRD patterns of NM and PAM modified NM are presented in Fig. 2a. Six characteristic peaks of Fe_3O_4 cubic space group (d-spacing = 2.96, 2.52, 2.09, 1.71, 1.61 and 1.48 Å) were observed, which, based on the standard pattern for Fe_3O_4, showed that the prepared samples were of high purity. The weaker diffraction peaks in the PAM modified NM compared to the NM alone indicate that the PAM modified the surface of the NM particles without changing their size (Song et al., 2014). Also, the FT-IR spectra of the PAM modified NM showed peaks at 582.41 and 628.83 cm^{-1} which confirm the Fe−O bonds and 3342 and 3419 cm^{-1} which belong to N−H stretching vibration. The 2855 and 2933 cm^{-1} peaks can be assigned to the stretch vibrations of the C−H bonds which originates from the PAM modified on the surface of NM particles. The absorption bond of 1668 cm^{-1} shows characteristic of NH_2 C=O and 1564 cm^{-1} representing the CN group (Fig. 2b). The size of the Fe_3O_4 particles coated by PAM were less than 30 nm (Fig. 2c).

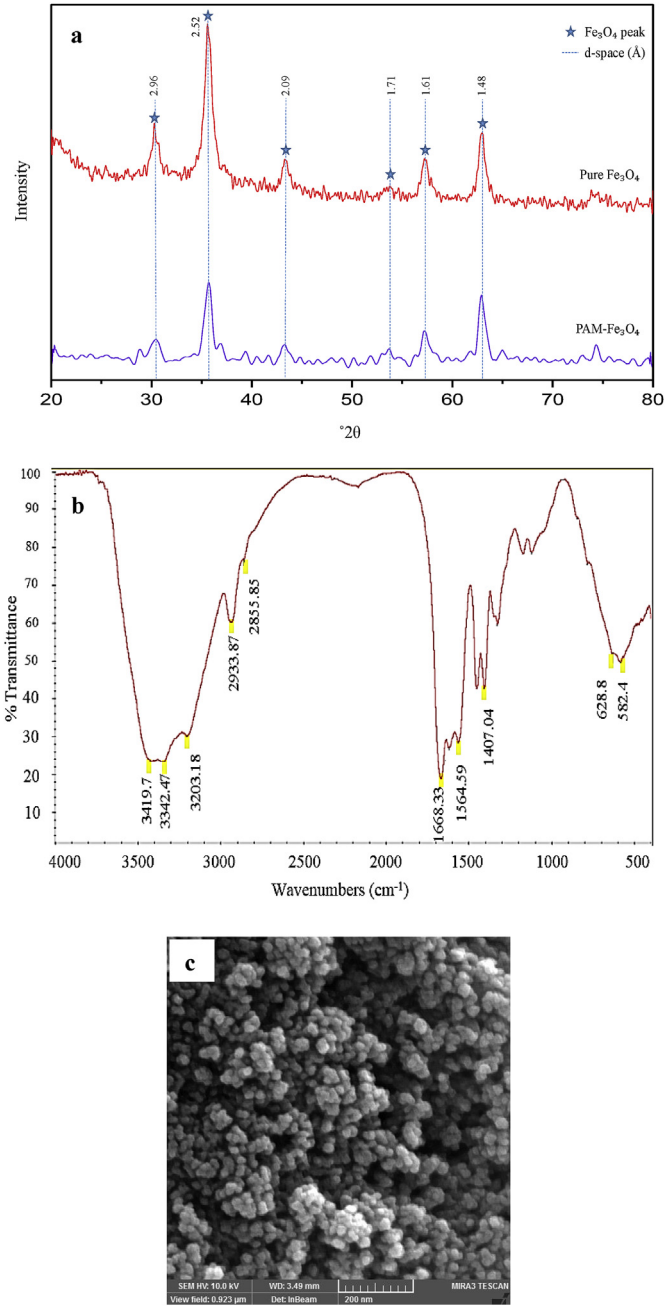

Fig. 2. (a) X-ray reflections of Fe_3O_4 (NM) and PAM-NM. (b) FT-IR spectra of PAM-NM. (c) Field-emission scanning electron micrograph of PAM-NM.

3.2. PAM and PAM-NM effects on soil aggregation

A PSD of 23% sand, 69% silt, and 8% clay (i.e., silt loam) was observed prior to treatment with PAM or PAM + NM particles. The SOC and initial soil water content was measured as 0.53% and 2.2%, respectively. The effect of the treatments can be seen within the upper 1 cm of the soil profile (Fig. 3). Aggregation of the soil particles in the first few millimeters below the soil surface was relatively low in the control largely due to deposition of fine particles by wind. The addition of PAM and PAM plus nanomagnetite treatments caused an increase in aggregation near the surface which coarsened the ASD within the upper 3 mm. Viscosity of the applied treatment is known to affect the depth penetration of PAM into the soil (Volk and Friedrich, 1980). High concentrations tend to impede the ability of the dissolved PAM to infiltrate the soil and cause a coarsening of the ASD near the surface

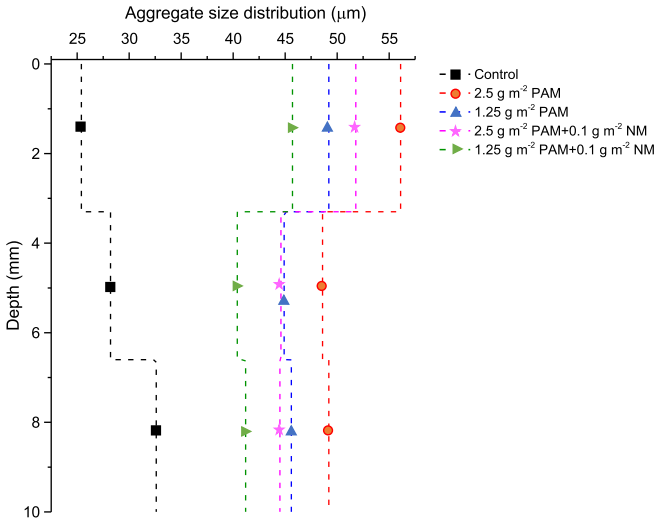

Fig. 3. Soil step function showing treatment effects on ASD 1 day after the start of the rainfall simulation.

compared to lower concentrations. This phenomenon can be observed in Fig. 3 where the mean aggregate diameter is coarser near the surface for the more concentrated PAM treatments. The addition of PAM-NM was not as effective in aggregating surface particles compared to PAM applications alone (Fig. 3). This can be attributed to the fact that binding of PAM with the magnetite nanoparticles reduces sites available for binding soil particles, thus, reducing the aggregation potential of the PAM (Zheng, 2011).

3.3. Runoff and sediment characteristics of PAM and PAM-NM treated soils

Several rainfall and water chemical parameters were measured prior to running the field experiment. The uniformity coefficient used for the simulated rainfall was an average of 93.7% which represents a high degree of spatial homogeneity during the experiment. Chemical properties of the water measured were pH (7.4), EC (1.04 dS m^{-1}), HCO_3^- (2.2 mol L^{-1}), Ca^{2+} (6.4 mol L^{-1}), Mg^{2+} (6.4 mol L^{-1}), Na^+ (4.3 mol L^{-1}), Cl^- (4.5 mol L^{-1}), and turbidity (0.08 NTU). The base cations measured were used to calculate an SAR of 2.4.

3.3.1. Runoff volume

Treatment effects on runoff volume are presented in Fig. 4 and

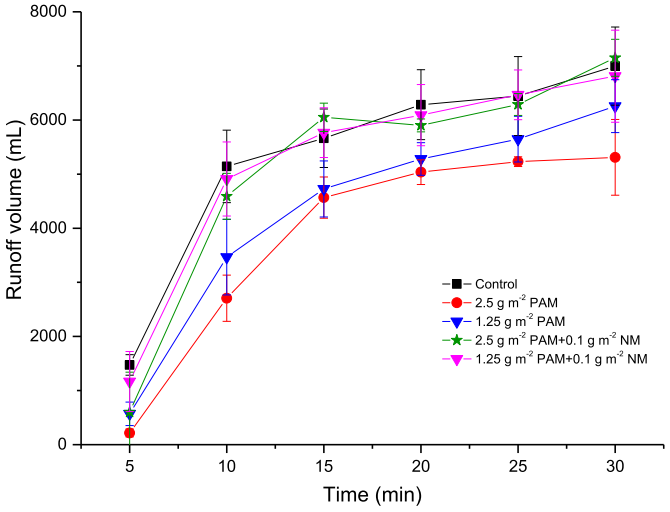

Fig. 4. Volume of runoff collected in the field during the 30-min simulated rainfall experiment.

Table 1
Measured values of runoff, sediment concentration and initial turbidity for different treatments.

Variable	PAM		PAM-Nano magnetite		Control
	1.25 g m^{-2}	2.5 g m^{-2}	1.25 g m^{-2} PAM +0.1 g m^{-2} NM	2.5 g m^{-2} PAM +0.1 g m^{-2} NM	
Total Runoff (L)	25.95a[b] (1.23[a])	23.07a (1.39[a])	31.21a (1.03[a])	30.58a (1.05[a])	32.00a
Sediment concentration (g/L)	0.57a (4.89[a])	0.47b (5.94[a])	0.77ac (3.62[a])	0.67c (4.16[a])	2.79d
Erosion rate (g m^{-2} min^{-1})	0.25a (5.96[a])	0.18b (8.28[a])	0.40c (3.73[a])	0.34d (4.38[a])	1.49e
Turbidity (NTU)	231.44a (2.57[a])	182.17b (3.27[a])	326.50c (1.83[a])	262.83c (2.27[a])	595.90c

[a] Mean average reduction of loss compared to control plot.
[b] Means followed by the same letters within a row are not significantly different at 5% of probability.

Table 1. Runoff volumes were not significantly different ($P > 0.05$) among the treatments and control (Zheng, 2011; Lee et al., 2011; Hayes et al., 2005; Li et al., 2014). During the experiments, runoff was observed approximately 2–4 min following the start of the simulated rainfall. Runoff was initiated in the control plots earlier than the PAM treated plots as also observed by Abu-Zreig (2006). As with runoff volume, we attribute these results to the effects of surface sealing and enhancement of rill formation at the surface of the control plots which limit the volume of infiltration (Martinez-Rodriguez et al., 2007; Abrol et al., 2013) due to a lack of enhanced soil physical quality as compared to the PAM treatments (Fig. 3).

3.3.2. Aggregate-size of the eroded sediment

PAM and PAM-NM significantly influenced the ASD of the eroded sediment. Fig. 5 shows that the addition of treatments increased the aggregate size of the sediment (1.4–1.8 times compared to the control). The runoff contained larger aggregate sizes for the PAM and PAM-NM treated plots during the first 10 min compared to the two later time intervals and control (Fig. 6a–c). This may be due to the high PAM concentration at the start of runoff initiation bonding with suspended soil particles and promoting flocculation (Zheng, 2011). Moreover, it seems that because stable aggregates increased under high PAM concentration near the soil surface, ASD of the sediment was closer to each other during the 3 time intervals (Fig. 6b).

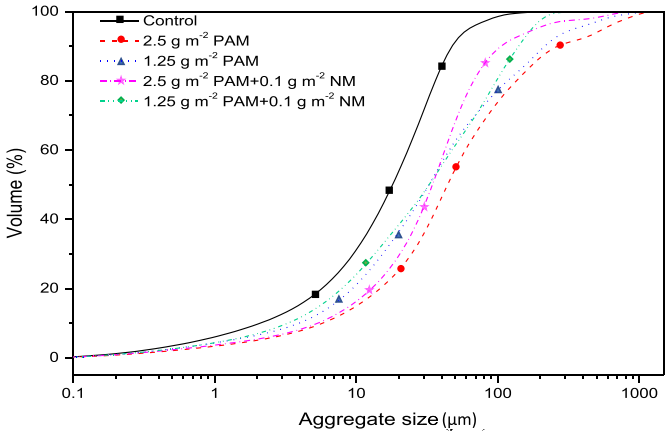

Fig. 5. Effect of PAM and PAM-NM treatments on aggregate-size distribution of the eroding sediment.

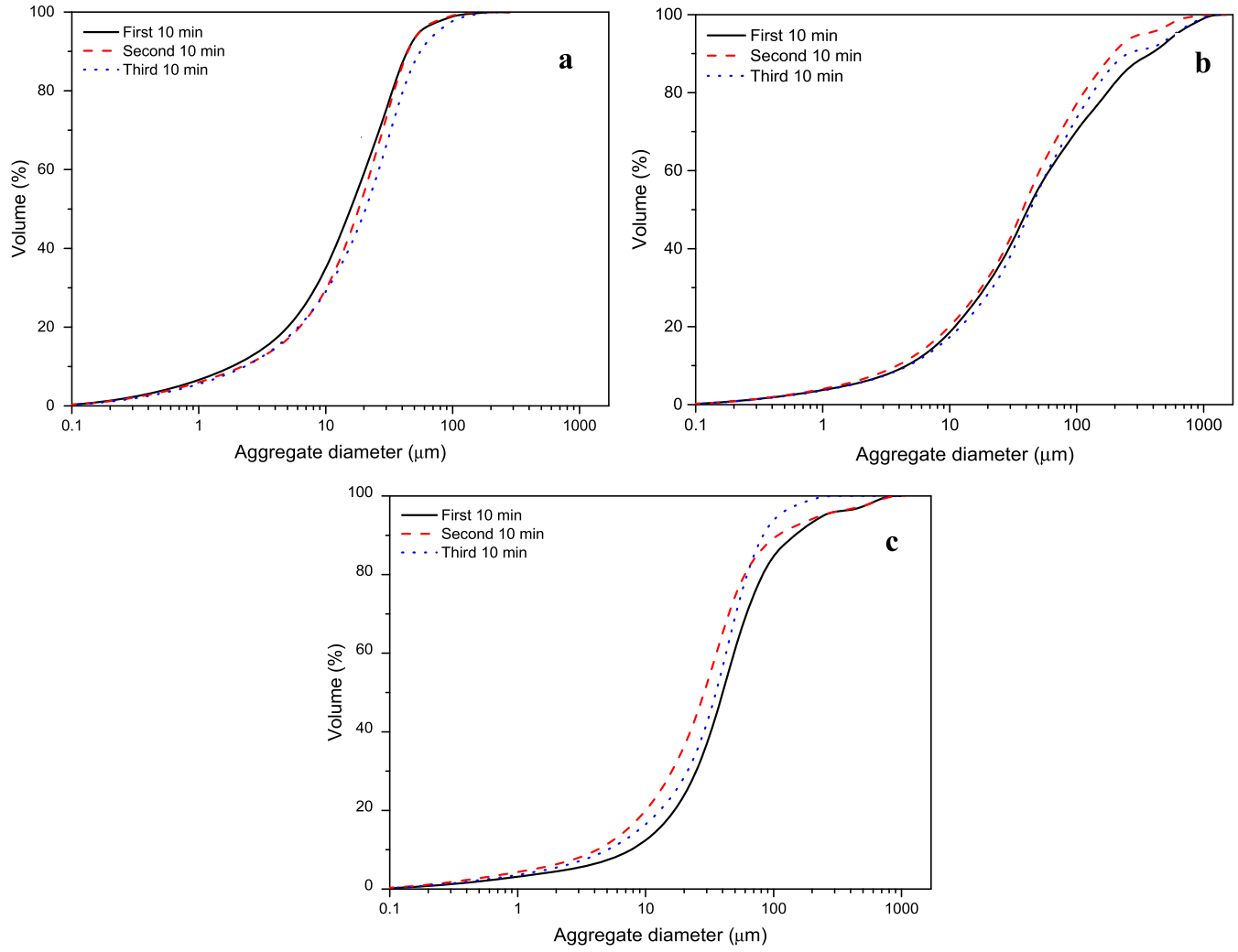

Fig. 6. Aggregate size for (a) control, (b) 2.5 g m^{-2} PAM, and (c) 2.5 g m^{-2} PAM + 0.1 g m^{-2} NM treated plots for three intervals over the course of the 30-min rainfall simulation experiment.

3.3.3. Erosion rate

The PAM and PAM-NM application was effective in reducing soil erosion. Soil erosion reduced by 6.0–8.3 and 3.7–4.4 times over the control for PAM and PAM-NM treatments, respectively (Table 1). This was due to the effect of PAM and PAM-NM on aggregate size which strongly affects erosion rates (Sajjadi and Mahmoodabadi, 2015). Aggregates are more resistant to erosive forces than individual particles and provide a surface roughness that aids deposition. These findings are similar to other studies that report on the effectiveness of PAM in reducing soil erosion (Sepaskhah and Shahabizad, 2010; Kang et al., 2014; White, 2006; McLaughlin and Brown, 2006).

3.4. PAM and PAM-NM effects on water quality

3.4.1. Manganese, phosphate and ammonium

Fig. 7a–c shows the volume of Mn^{2+}, PO_4^{3-}-P, and NH_4^+-N losses measured from three intervals over the course of the 30-min rainfall simulation experiment. During the experiment, mass loadings of Mn^{2+}, PO_4^{3-}-P, and NH_4^+-N from the control were high with average concentrations of 635.3 μg L^{-1}, 4.9 mg L^{-1}, and 1.2 mg L^{-1}, respectively. Manganese, PO_4^{3-}-P and NH_4^+-N losses from each rainfall event were affected by PAM treatments. However, the combination of PAM-NM was more effective at controlling PO_4^{3-}-P and Mn^{2+} from runoff, likely due to sorption characteristics of the nanoparticles due to their small size, higher specific surface area, and enhanced surface reactivity. Nutrient losses from PAM and PAM-NM treatments were reduced on average 32.2 and 151.9 fold for Mn^{2+}, 1.8 and 2.7 fold for PO_4^{3-}-P, and 2.3 and 1.6 fold for NH_4^+-N over the control, respectively. Moreover, Mn^{2+} and PO_4^{3-}-P losses were reduced in the PAM-NM treatments on average 4.7 and 1.5 times compared to the PAM mono-application, respectively. The results showed the reduction of Mn^{2+} concentration to less than 100 μg L^{-1} (under the threshold of neurotoxicity of Mn^{2+} in children, Khan et al., 2012), especially at high concentrations of NM particles. As a consequence, PAM-NM might be an important soil amendment for reducing the transport of Mn^{2+} and PO_4^{3-} in runoff. Furthermore, PO_4^{3-} concentrations decrease with time due to high accumulation of PO_4^{3-} at shallow depths and transport by surface runoff (Runge and Riecken, 1966; Schoumans, 2015). Although the positive effect of PAM on nutrient retention has been reported by other researchers (Busscher et al., 2007; Jiang et al., 2010; Kim et al., 2015; Ao et al., 2018), there appears to be no information on the use of PAM-modified NM particles for nutrient and Mn^{2+} retention in soil.

3.4.2. Sediment concentration in runoff

Table 1 shows that both PAM and PAM-NM treatments significantly ($P < 0.05$) reduced runoff-generated sediment during the simulated rainfall compared to the control. As PAM content increased, runoff-generated sediment decreased reaching less than 0.5 g L^{-1} for the 2.5 g m^{-2} PAM amendment (Table 1; Fig. 8a). The sediment concentration in the runoff from the control plots increased rapidly to

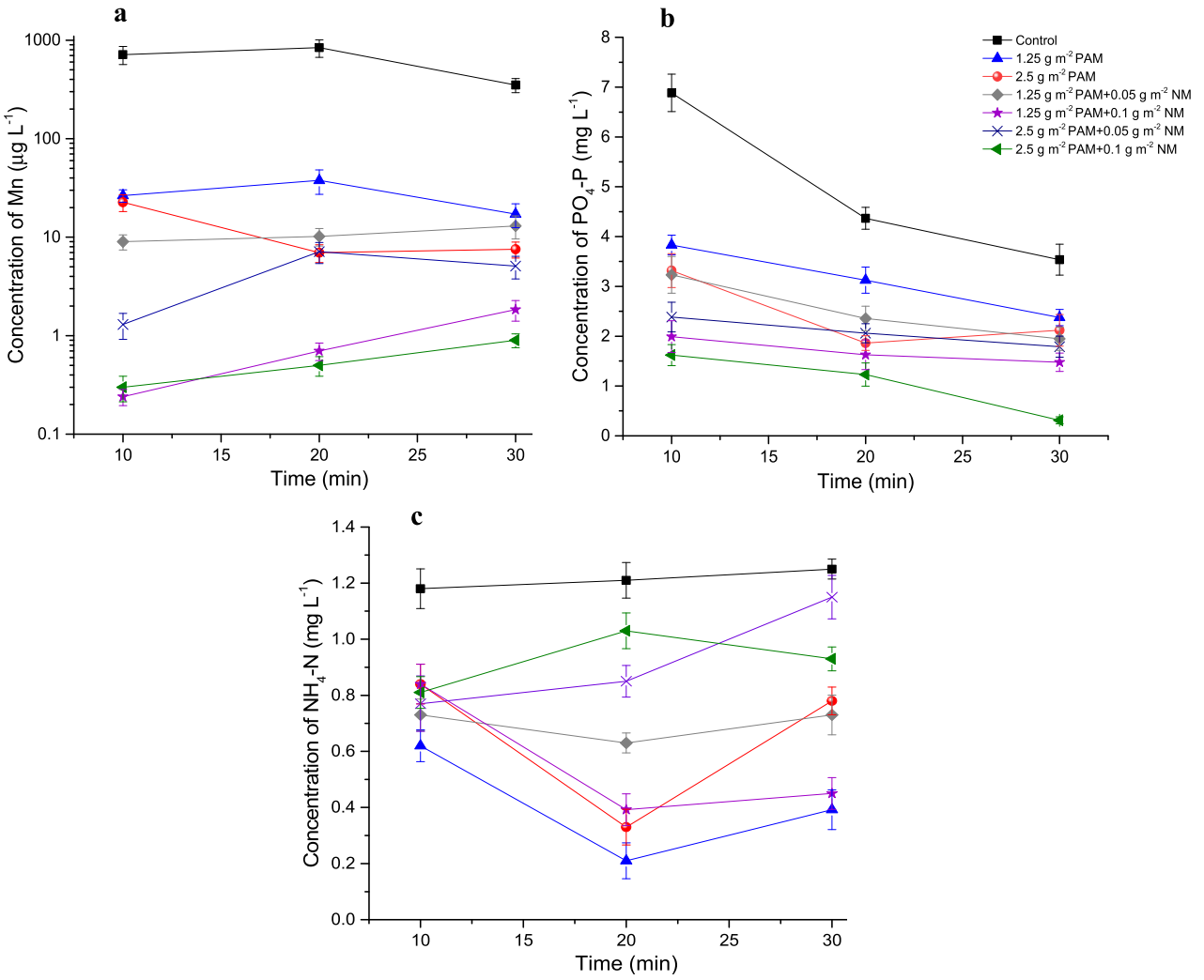

Fig. 7. Concentrations of (a) Mn^{2+}, (b) PO_4^{3-}-P, and (c) NH_4^{+}-N in the runoff water over the course of the 30-min rainfall simulation experiment.

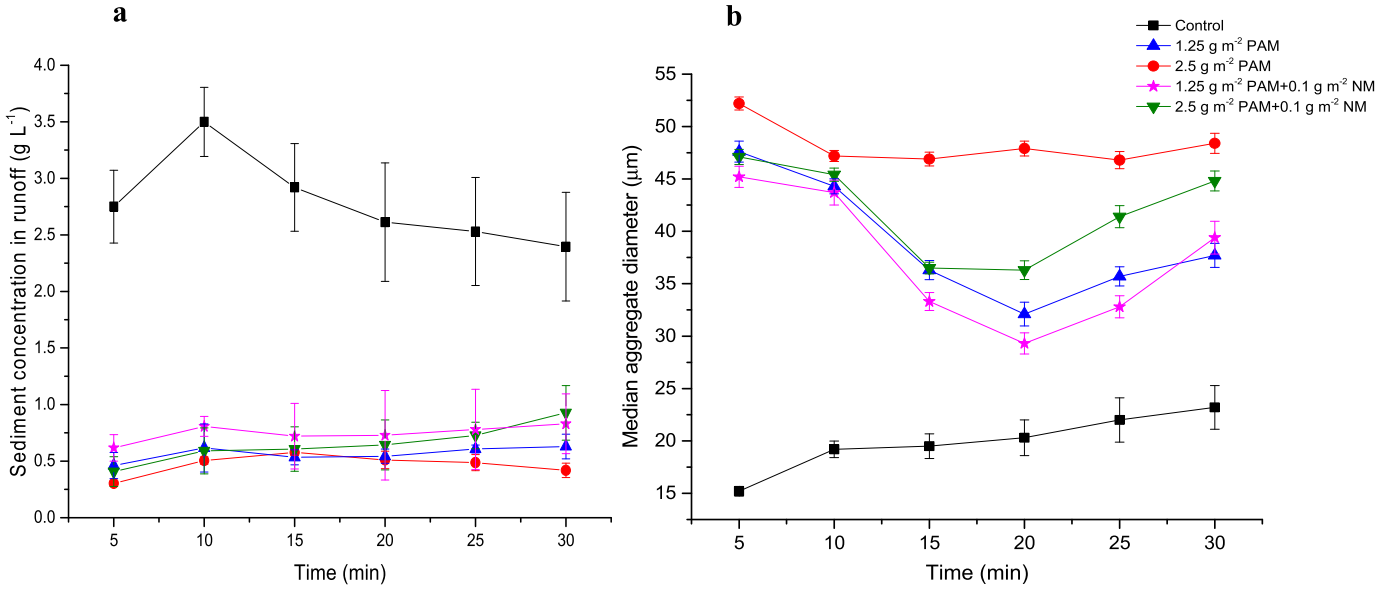

Fig. 8. (a) Concentration and (b) median aggregate diameter of sediment in the runoff water monitored for the duration of the rainfall simulation experiment.

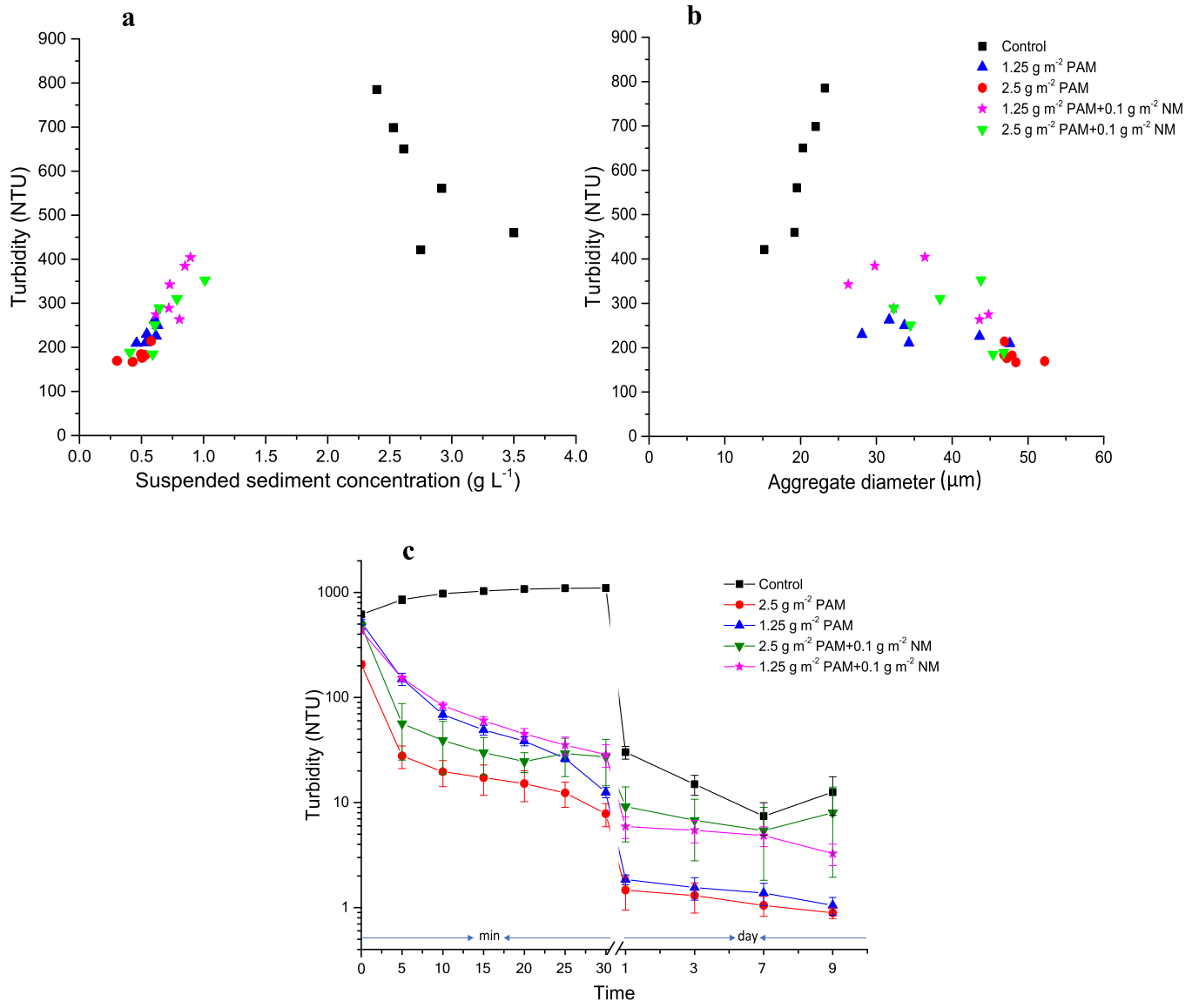

Fig. 9. (a) Relation between turbidity and suspended sediment concentration, (b) suspended aggregate size, and (c) turbidity kinetics of runoff for control and treated plots under stagnant conditions.

3.5 g L^{-1} during the first 10 min, decreased slowly thereafter, and reached 2.4 g L^{-1} by the end of the rainfall simulation run (Fig. 8a). The increase in sediment concentration in the first 10 min is mainly due to the presence of fine soil particles at the land surface (Fig. 3). The uplift force from the flow of runoff water tends to entrain fine soil particles into the suspension during the first 10 min (Fig. 8b). The decrease in sediment concentration in the control after 10 min may have been caused by the coarsening of the ASD with depth stabilizing the sediment against runoff (Fig. 3). Furthermore, the decreasing sediment concentration with time for the high PAM treatments was attributed to the clustering effect of these treatments on soil particles (Figs. 8b and 5). These aggregates accumulated behind the plant residue and formed micro-terraces thereby protecting them from further transport. The average sediment concentrations of the runoff in the plots treated with 1.25 g m^{-2} and 2.5 g m^{-2} PAM were reduced by 4.9 and 5.9 times compared to the control plots, respectively. These findings are consistent with similar studies where significant reduction in sediment yield was observed (Zhang et al., 1998; Blanco-Canqui et al., 2004; Ao et al., 2016; Babcock and McLaughlin, 2011).

We observed a slightly lower reduction in runoff sediment concentration compared to the control for low and high concentrations of PAM-NM (3.6 and 4.2 times, respectively) (Table 1). We attribute this slight lowering of effectiveness in soil erosion control potential to the binding of PAM molecules with the nanoparticles reducing the ability for PAM to bind with soil particles (Zheng, 2011).

3.4.3. Turbidity

Table 1 shows that the average turbidity of the runoff in treated plots was lower than the control during the 30-min rainfall simulation experiment with average turbidity reductions of 2.6, 3.3, 1.8 and 2.3 fold over the control, for the low and high concentration PAM-only treatments and the low and high concentration PAM-NM treatments, respectively. As PAM application rates decreased, turbidity measurements increased. The addition of NM slightly decreased the influence of the PAM in affecting turbidity compared to the control. Average turbidity kinetics of the runoff samples indicate that the potential turbidity for runoff when directed into a relatively quiescent basin with stagnant conditions prior to discharge would decrease for all treatments. For the control plots, turbidity stayed relatively consistent for 30 min followed by a slower decrease compared to the treatments (Fig. 9c). This is because turbidity depends generally on the suspended sediment concentration and suspended aggregate size (Fig. 9a and b). These

treatments caused fine particles to aggregate leading to the deposition of particles and reduction of turbidity. It can be seen that final measurements for PAM-only treatments reached the lowest turbidity levels of around 1 NTU after 10 days. The PAM effect on turbidity present in both the PAM only and PAM-NM treatments is important, as it may help to reduce turbidity in outflows of basins, increase water quality, and prevent decreasing water-storage capacity of dams (Shoemaker, 2009; Zheng, 2011). Our findings are on the order of values reported by Zheng (2011) who treated 12 × 36-in plots with 0.3% PAM and 0.3% PAM + stabilized NM (0.1 g L^{-1} as Fe), and observed an average turbidity reduction of 89% and 83%, respectively.

4. Conclusions

In this study, we implemented a combination of PAM and NM and evaluated its potential to reduce soil erosion and pollutant loads compared to PAM-only treatments in field plots in an important region in Iran. Our results demonstrate reductions in runoff volume, average concentrations of sediment, turbidity, and concentrations of Mn^{2+}, PO_4^{3-}-P and NH_4^+-N in runoff during the rainfall simulation. The combination of PAM and NM especially at high concentrations of NM (0.1 g m^{-2}) was effective in controlling Mn^{2+} and PO_4^{3-}-P from runoff. Moreover, PAM significantly affected the ASD of the eroded sediment, coarsening the distribution. Coarser aggregates were resistant to detachment or accumulated behind surface plant residues leading to lower erosion rates. We observed considerable reduction in surface erosion from the PAM-NM treatment which is important for preventing sedimentation of dammed water reservoirs and improving overall water quality. We expect that the results of this study will be useful in developing PAM-modified NM adsorbents that can be used for the simultaneous in situ control of soil erosion and contaminant transport (Mn^{2+}, PO_4^{3-}-P and NH_4^+-N) for this region of Iran.

Author information

The authors declare no competing financial interest.

Acknowledgments

The authors are grateful to Dr. Stephan Opitz (Laboratory for Physical Geography, University of Cologne) for valuable support in laboratory analyses and discussion of data. We also thank Dr. Vahedberdi Sheikh (Department of Watershed Management, Gorgan University of Agricultural Sciences and Natural Resources) for providing us with rainfall simulator.

References

Abrol, V., Shainberg, I., Lado, M., Ben-Hur, M., 2013. Efficacy of dry granular anionic polyacrylamide (PAM) on infiltration, runoff and erosion. Eur. J. Soil Sci. 64 (5), 699–705. http://dx.doi.org/10.1111/ejss.12076.

Abu-Zreig, M., 2006. Runoff and erosion control of silt clay soil with land application of polyacrylamide: (Abfluss-und Erosionsregulierung eines sandigen Lehmbodens durch Anwendung von Polyacrylamid). Arch. Agron Soil Sci. 52 (3), 289–298. http://dx.doi.org/10.1080/03650340600572637.

Agheli-e Kohneshari, L., Sadeghi, H., 2005. Estimating the economic impacts of soil erosion in Iran. Q. J. Econom. Res. 15, 87–100.

Ajwa, H.A., Trout, T.J., 2006. Polyacrylamide and water quality effects on infiltration in sandy loam soils. Soil Sci. Soc. Am. J. 70 (2), 643–650. http://dx.doi.org/10.2136/sssaj2005.0079.

Alizadeh, A., 1995. Principles of Applied Hydrology. Emam Reza Press, Mashhad, Iran.

Ao, C., Yang, P., Ren, S., Xing, W., Li, X., Feng, X., 2016. Efficacy of granular polyacrylamide on runoff, erosion and nitrogen loss at loess slope under rainfall simulation. Environ. Earth Sci. 75 (6), 490. http://dx.doi.org/10.1007/s12665-015-5110-3.

Ao, C., Yang, P., Ren, S., Xing, W., 2018. Mathematical model of ammonium nitrogen transport with overland flow on a slope after polyacrylamide application. Sci. Rep. 8 (1), 6380. http://dx.doi.org/10.1038/s41598-018-24819-9. 2018 - Nature.com.

AQUASTAT, 2008. Country Fact Sheet: Iran. FAO's Global Information System on Water and Agriculture.

Babcock, D.L., McLaughlin, R.A., 2011. Runoff water quality and vegetative establishment for ground covers on steep slopes. J. Soil Water Conserv. 66 (2), 132–141. http://dx.doi.org/10.2489/jswc.66.2.132.

Barvenik, F.W., 1994. Polyacrylamide characteristics related to soil applications. Soil Sci. 158, 235–243.

Blanco, H., Lal, R., 2008. Principles of Soil Conservation and Management. Springer, Heidelberg, Germany.

Blanco-Canqui, H., Gantzer, C.J., Anderson, S.H., Thompson, A.L., 2004. Soil berms as an alternative to steel plate borders for runoff plots. Soil Sci. Soc. Am. J. 68, 1689–1694.

Busscher, W.J., Novak, J.M., Caesar-TonThat, T.C., 2007. Organic matter and polyacrylamide amendment of Norfolk loamy sand. Soil Tillage Res. 93 (1), 171–178.

Christiansen, J.E., 1942. Irrigation by Sprinkling. University of California press, Berkeley, California.

Dabbous, B.A., 1962. Study of Sprinkler Uniformity Evaluation Methods. Master thesis. Utah state University, Logan, Utah.

Engleman, E.E., Jackson, L.L., Norton, D.R., 1985. Determination of carbonate carbon in geological materials by coulometric titration. Chem. Geol. 53 (1–2), 125–128.

Entry, J.A., Sojka, R.E., Watwood, M., Ross, C., 2002. Polyacrylamide preparations for protection of water quality threatened by agricultural runoff contaminants. Environ. Pollut. 120, 191–200.

ESRD (Alberta Environment and Sustainable Resource Development), 2014. Environmental Quality Guidelines for Alberta Surface Water. Water Policy Branch, Policy Division. Edmonton. pp. 48.

Fu, B.J., Chen, L.D., 2000. Agricultural landscape spatial pattern analysis in the semi-arid hill area of the Loess Plateau, China. J. Arid Environ. 44, 291–303.

Green, V.S., Stott, D.E., Norton, L.D., Graveel, J.G., 2000. PAM molecular weight and charge effects on infiltration under simulated rainfall. Soil Sci. Soc. Am. J. 64, 1786–1791.

Guzzo, J., Guezennec, A.G., 2015. Degradation and transfer of polyacrylamide based flocculent in sludge and industrial and natural waters. Environ. Sci. Pollut. Res. 22 (9), 6387–6389.

Hayes, S.A., McLaughlin, R.A., Osmond, D.I., 2005. Polyacrylamide use for erosion and turbidity control on construction sites. J. Soil Water Conserv. 60, 193–199.

He, F., Zhao, D.Y., 2005. Preparation and characterization of a new class of starch-stabilized bimetallic nanoparticles for degradation of chlorinated hydrocarbons in water. Environ. Sci. Technol. 39, 3314–3326.

He, F., Zhao, D.Y., Liu, J.C., Roberts, C.B., 2007. Stabilization of Fe-Pd nanoparticles with sodium carboxymethyl cellulose for enhanced transport and dechlorination of trichloroethylene in soil and groundwater. Ind. Eng. Chem. Res. 46, 29–34.

Heydarizad, M., 2018. Hydrochemical assessment and quality classification of water in Torogh and Kardeh dam reservoirs, North-East Iran. Int. J. Environ. Ecol. Engin. 12 (1), 49–53.

ICOLD Committee on Reservoir Sedimentation, March 2009. Sedimentation and Sustainable Use of Reservoirs and River Systems. grbasson@sun.ac.za.

Jackson, L.L., Roof, S.R., 1992. Determination of the forms of carbon in geologic materials. Geostand. Newsl. 16 (2), 317–323.

Jahanjo, B., 2000. The Chemical Effect of Polyacrylamide on the Diffusion and Soil Erosion Control in the Irrigation. M.Sc. Dissertation. Tehran University, Tehran, Iran.

Jennings, E., Mills, P., Jordan, P., Jensen, J.P., Barr, A., Glasgow, G., Irvine, K., 2003. Eutrophication from Agricultural Sources: Seasonal Patterns and Effects of Phosphorus. Environmental RTDI Programme 2000-2006. Final report.

Jiang, T., Teng, L., Wei, S., Deng, L., Luo, Z., Chen, Y., Flanagan, D.C., 2010. Application of polyacrylamide to reduce phosphorus losses from a Chinese purple soil: a laboratory and field investigation. J. Environ. Manag. 91, 1437–1445.

Kang, J., Amoozegar, A., Heitman, J.L., McLaughlin, R.A., 2014. Granular and dissolved polyacrylamide effects on erosion and runoff under simulated rainfall. J. Environ. Qual. 43, 1972–1979.

Khan, K., Wasserman, G.A., Liu, X., Ahmed, E., Parvez, F., Slavkovich, V., Levy, D., Mey, J., van Geen, A., Graziano, J.H., Factor-Litvak, P., 2012. Manganese exposure from drinking water and children's academic achievement. Neurotoxicology 33 (1), 91–97.

Kim, M., Song, I., Kim, M., Kim, S., Kim, Y., Choi, Y., Seo, M., 2015. Effect of polyacrylamide application on water and nutrient movements in soils. J. Agric. Chem. Environ. 4, 76–81.

Klopfenstein, S.T., Hirmas, D.R., Johnson, W.C., 2015. Pedogenesis along a climosequence in loess-derived soils of the central Great Plains, USA. Catena 133, 25–54.

Kurenkov, V.F., Myagchenkov, V.A., 1996. In: In: Salamon, J.C. (Ed.), Polymeric Materials Encyclopedia, vol. 1. CRC press, pp. 47–61.

Lee, S.S., Gantzer, C.J., Thompson, A.L., Anderson, S.H., 2011. Polyacrylamide and gypsum amendments for erosion and runoff control on two soil series. J. Soil Water Conserv. 66 (3), 172–177.

Li, F., Wang, A., Wu, L.S., 2014. Interaction effects of polyacrylamide application rate, molecular weight, and slope gradient on runoff and soil loss under sprinkler irrigation. Adv. Mater. Res. 955–959, 3489–3498.

Liang, Q., An, B., Zhao, D., 2013. Removal and immobilization of arsenic in water and soil using Polysaccharide-modified magnetite nanoparticles. Chapter 12 In: Ahuja, S. (Ed.), Monitoring Water Quality. Pollution Assessment, Analysis and Remediation. Elsevier Inc. Environmental engineering program, department of civil engineering, Auburn University, Auburn, Al, USA.

Mafongoya, P.L., Bationo, A., Kihara, J., Waswa, B.S., 2006. Appropriate technologies to replenish soil fertility in southern Africa. Nutrient Cycl. Agroecosyst. 76, 137–151.

Mamedov, A.I., Beckmann, S., Huang, C., Levy, G.J., 2007. Aggregate stability as affected by polyacrylamide molecular weight, soil texture and water quality. Soil Sci. Soc. Am. J. 71, 1909–1918.

Martinez-Rodriguez, G.A., Vazquez, M.A., Guzman, J.L., Ramos-Santana, R., Santana, O., 2007. Use of polyacrylamide as an erosion control strategy in a highly eroded soil of Puerto Rico. J. Agric. Univ. Puert. Rico 91, 87–100.

McLaughlin, R.A., Bartholomew, N., 2007. Effects of polyacrylamide and soil properties on flocculation. Soil Sci. Soc. Am. J. 71, 537–544.
McLaughlin, R.A., Brown, T.T., 2006. Evaluation of erosion control products with and without added polyacrylamide. J. Am. water res. assoc. 42, 675–684. http://dx.doi.org/10.1111/j. 1752-1688.
McTainsh, G.H., Nickling, W.G., Lynch, A.W., 1997. Dust deposition and particle size in Mali, West Africa. Catena 29, 307–322.
Noor, H., Fazli, S., Alibakhshi, S.M., 2013. Evaluation of the relationships between runoff-rainfall sediment related nutrient loss (A case study: Kojour Watershed, Iran). Soil Water Res. 8 (4), 172–177.
Orts, W.J., Roa-Espinosa, A., Sojka, R.E., Glenn, G.M., Imam, S.H., Erlacher, K., Pedersen, J., 2007. Use of synthetic polymers and biopolymers for soil stabilization in agricultural, construction and military applications. J. Mater. Civ. Eng. 19 (1), 58–66.
Rahmanian, M.R., Banihashemi, M.A., 2011. Sediment distribution pattern in some Iranian dams based on a new empirical reservoir shape function. Lake Reservoir Manag. 27, 245–255.
Reimer, P.S., 1999. Environmental Effects of Manganese and Proposed Freshwater Guidelines to Protect Aquatic Life in British Colombia. Department of Chemical and Bio-Resource Engineering, University of British Columbia.
Runge, E.C.A., Riecken, F.F., 1966. Influence of natural drainage on the distribution and forms of phosphorus in some Iowa Prairie soils. Soil Sci. Soc. Am. Proc. 30, 624–630.
Sadalmelik, 2007. Topographic Map of Iran. Created with GMT from SRTM Data.
Sajjadi, S.A., Mahmoodabadi, M., 2015. Aggregate breakdown and surface seal development influenced by rain intensity, slope gradient and soil particle size. Solid Earth 6, 311–321. http://dx.doi.org/10.5194/se-6-311-2015.
Schoumans, O.F., 2015. Phosphorus Leaching from Soils: Process Description, Risk Assessment and Mitigation. PhD thesis. Wageningen University, Wageningen, NL, pp. 261 ISBN 978-94-6257-299-7.
Schwertmann, U., Cornell, R.M., 2000. Iron Oxide in the Laboratory; Preparation and Characterization. Wiley-vch, Weinheim, Germany.
Sepaskhah, A.R., Shahabizad, V., 2010. Effects of water quality and PAM application rate on the control of soil erosion, water infiltration and runoff for different soil textures measured in a rainfall simulator. Biosyst. Eng. 106, 513–520.
Seybold, C.A., 1994. Polyacrylamide review: soil conditioning and environmental fate. Commun. Soil Sci. Plant Anal. 25, 2171–2185.
Shoemaker, A.E., 2009. Evaluation of Anionic Polyacrylamide as an Erosion Control Measure Using Intermediate-scale Experimental Procedures. Master Thesis. Auburn University, USA, pp. 220.
Sivapalan, S., 2006. Some benefits of treating a sandy soil with a crosslinked-type polyacrylamide. Aust. J. Exp. Agric. 46, 579–584.
Soil Survey Staff, 2014. Keys to Soil Taxonomy, twelfth ed. USDA-NRCS, Washington DC.
Sojka, R.E., Bjorneberg, D.L., Entry, J.A., Lentz, R.D., Orts, W.J., 2007. Polyacrylamide in agriculture and environmental land management. Adv. Agron. 92, 75–162.
Sojka, R.E., Entry, J.A., 2000. Influence of polyacrylamide application to soil on movement of microorganisms in runoff water. Environ. Pollut. 108, 405–412.
Sojka, R.E., Orts, W.J., Entry, J.A., 2004. Soil physics and hydrology: conditioners. In: Hillel, D. (Ed.), Encyclopedia of Soil Science. Elsevier, academic press, Oxford, U.K, pp. 301–306p.
Song, W., Liu, M., Hub, R., Tan, X., Li, J., 2014. Water-soluble polyacrylamide coated-Fe_3O_4 magnetic composites for high-efficient enrichment of U(VI) from radioactive wastewater. Chem. Eng. J. 246, 268–276.
Sparks, D.L., 2007. Advances in Agronomy, vol. 92 Academic Press ISBN: 0080469191, 9780080469195.
Sparks, D.L., 2003. Environmental Soil Chemistry. Academic Press, New York.
Street, A., Sustich, R., Duncan, J., Savage, N., 2014. Nanotechnology Applications for Clean Water: Solutions for Improving Water Quality, 2th Edition. William Andrew, pp. 704 ISBN: 1455731854, 9781455731855.
Tabrizi, N., Ghorbani, A., 2013. Monitoring water quality in Torogh dam reservoir, NE Iran. In: The National Zagros Environmental hazard Conference, Khoramabad, Iran, in Persian.
Uwimana, A., van Dam, A., Gettel, G., Bigirimana, B., Irvine, K., 2017. Effects of river discharge and land use and land cover (LULC) on water quality dynamics in migina catchment, Rwanda. Environ. manage. 60 (3), 496–512.
Volk, H., Friedrich, R.E., 1980. Polyacrylamide. In: Davidson, R.L. (Ed.), Handbook of Water Soluble Gums and Resins. McGraw Hill 16-1 – 16-26.
Weston, D.P., Lentz, R.D., Cahn, M.D., Ogle, R.S., Rothert, A.K., Lydy, M.J., 2009. Toxicity of anionic polyacrylamide formulations when used for erosion control in agriculture. J. Environ. Qual. 38, 238–247.
White, R.E., 2006. Principles and Practices of Soil Science. The Soil as a Natural Resource, fourth ed. Blackwell Publishing, Oxford, U.K.
Wisser, D., Frolking, S., Hagen, S., Bierkens, M.F.P., 2013. Beyond peak reservoir storage? A global estimate of declining water storage capacity in large reservoirs. Water Resour. Res. 49, 5732–5739. http://dx.doi.org/10.1002/wrcr.20452.
Wu, W., He, Q., Jiang, C., 2008. Magnetic iron oxide nanoparticles: synthesis and surface functionalization strategies. Nanoscale Res. Lett. 3 (11), 397–415.
Zhang, X.C., Miller, W.P., Nearing, M.A., Norton, L.D., 1998. Effects of surface treatment on surface sealing, runoff, and interrill erosion. Trans. of the ASAE 41, 989–994.
Zhang, Z., Li, M., Chen, W., Zhu, S., Liu, N., Zhu, L., 2010. Immobilization of lead and cadmium from aqueous solution and contaminated sediment using nano-hydroxyapatite. Environ. Pollut. 158 (2), 514–519.
Zheng, M.A., 2011. Technology for Enhanced Control of Erosion, Sediment and Metal Leaching at Disturbed Land Using Polyacrylamide and Magnetite Nanoparticles. Master thesis. Auburn University, Auburn, Alabama.